Available online at www.sciencedirect.com
ScienceDirect
Scripta Materialia 58 (2008) 53–56
Scripta MATERIALIA
www.elsevier.com/locate/scriptamat

Structural stability of ultrafine-grained copper

Y.J. Li,[a,*] R. Kapoor,[b] J.T. Wang[c] and W. Blum[a]

[a]*Department of Materials Science and Engineering, Institute I: General Materials Properties WW I, University of Erlangen-Nürnberg, Martensstr. 5, 91058 Erlangen, Germany*
[b]*Materials Science Division, Bhabha Atomic Research Centre, Mumbai 400085, India*
[c]*School of Materials Science and Engineering, Nanjing University of Science and Technology, Nanjing 210094, China*

Received 27 June 2007; revised 27 August 2007; accepted 30 August 2007
Available online 1 October 2007

Ultrafine-grained (UFG) pure Cu, produced by equal channel angular pressing, was subjected to thermomechanical treatment (TMT) with stepwise deformation at rising temperature. The TMT leads to homogeneous subgrain coarsening according to the established inverse relation between flow stress and steady-state subgrain size and retards static recrystallization during annealing at 403 K.

Keywords: Ultrafine-grained Cu; Work softening; Subgrain coarsening; Grain boundary; Thermomechanical treatment

Pure ultrafine-grained (UFG) Cu produced by severe plastic deformation (SPD) has unique and useful mechanical properties, including high values of work hardening rate, yield stress and strain rate sensitivity of flow stress (see e.g. [1–5]). Its cellular/subgrain microstructure, resulting from storage and dynamic recovery of dislocations, is typical of cold-worked materials [6]. Each subgrain has a number of different boundaries equal to the number of its next neighbors. Depending on the misorientation ϕ of the neighbors, the boundaries of a subgrain have low-angle (network of lattice dislocations, $\phi < 15°$) or high-angle boundaries ($\phi > 15°$). The volume density of the subgrain boundary area is f_w/w, where w is the linear intercept of the subgrains; the geometrical factor $f_w \approx 2$ as the subgrains are approximately equiaxed. Analogously, the volume density of the high-angle boundary area is f_d/d. The area fraction of high-angle boundaries is $f_{\mathrm{hab}} = (f_d/f_w)(w/d)$ and may be approximated as w/d because the deviation of the geometrical factor f_d from 2 is limited. Substantial differences in f_{hab} may result in significant changes in the mechanical properties of a material due to the significant differences between the low- and high-angle boundaries. In particular, low-angle boundaries are penetrable dislocation obstacles, in contrast to (in general) high-angle boundaries, and the diffusivity of high-angle boundaries is much larger than that of low-angle ones.

The special properties of UFG materials result from a relatively large f_{hab}. The high amount of stored energy restricts the stability of UFG materials against thermally activated structural changes. For instance, discontinuous static recrystallization occurs at relatively low homologous temperatures [6]. When the recrystallized volume is sufficiently large, hardness and yield stress are significantly reduced. Work softening during deformation of UFG materials at temperatures above the SPD processing temperature T_{SPD} has also been observed; examples are given in Li et al. [3] and Figure 1. The softening shows up as a decrease in flow stress σ at constant (total) deformation rate $\dot{\varepsilon}_{\mathrm{tot}}$ and as an increase in creep rate $\dot{\varepsilon}$ at constant stress σ. The microstructural origin of work softening is not yet known in detail. Li et al. proposed homogeneous coarsening of the subgrain structure and a resulting increase of subgrain size [3]. However, some kind of dynamic recrystallization cannot be excluded as a cause of softening.

Strategies to stabilize the UFG structure by thermal treatments and to modify it in order to optimize its mechanical properties have been proposed [7–9]. These approaches comprise partial recrystallization to form a bimodal structure. Li et al. [3] reported that a thermomechanical treatment (TMT) stabilizes UFG Cu.

In the present work, we report on the stabilization of UFG Cu by TMT and its microstructural origin. UFG Cu (99.98 wt.%, oxygen-free high-conductivity) was

* Corresponding author. Tel.: +49 9131 8527486; fax: +49 9131 8527504; e-mail: Yujiao.li@ww.uni-erlangen.de

1359-6462/$ - see front matter
doi:10.1016/j.scriptamat.2007.08.033

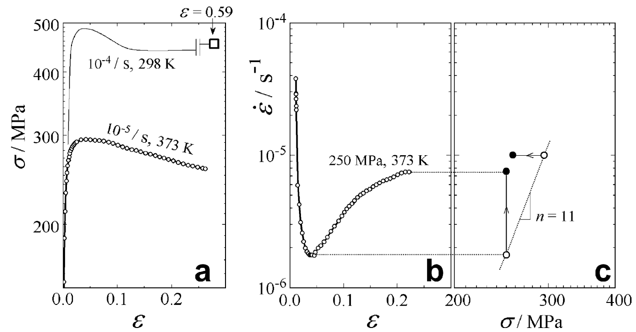

Figure 1. Work softening of UFG Cu during uniaxial compression at 373 K and (a) constant $\dot{\varepsilon}_{tot}$, (b) constant σ, (c) deformation paths in (a) and (b) in $\dot{\varepsilon}$–σ field from maximum of deformation resistance (open circles) to end of tests (filled circles); n is the σ-exponent of $\dot{\varepsilon}$ at the maximum deformation resistance (estimated error ±4). The curve for 298 K (thin line) in (a) was taken from Ref. [17] for UFG Cu produced by cryorolling at 77 K and deformed at room temperature.

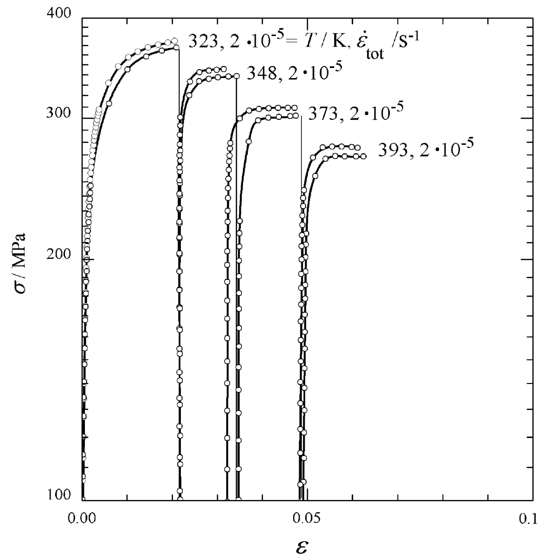

Figure 2. σ–ε curves during TMT of UFG Cu at successively increasing T; upper and lower curves correspond to two specimens of slightly different strength.

produced from material with initial grain size ≈2 mm by equal channel angular pressing (ECAP) for eight passes through route B_C (rotation of sample by 90° in the same direction after each pass [10]). The subgrain size of the UFG Cu is $w_0 = 0.28$ μm [11]. The fraction of high-angle boundaries was found to be around 0.6 (Y. Zhang, unpublished); this agrees with the literature [6,12–14], which reports $0.5 < f_{hab} < 0.7$. Deformation tests on UFG Cu were performed with an Instron 4505 testing machine at elevated temperatures $323\ K \leqslant T \leqslant 403\ K$ in uniaxial compression under strain rate control and stress control (creep). Temperature was established by heating without load at the rate $\dot{T} = 7\ K\ min^{-1}$ and soaking for 0.5 h before deformation was started. The direction of compression was parallel to the ECAP direction. The initial shape factor (ratio of length to square root of cross-section) of the sample was 1.3. Stress σ was determined as force per average cross-section at T (calculated with thermal expansion coefficient of $1.7 \times 10^{-5} K^{-1}$). The (true) total (elastic plus inelastic) strain ε_{tot} was determined by measuring the change of length by extensometers attached to the deformation machine at a small distance from the test specimen. Due to the relatively large shape factor and the limited strains, correction of σ for the effect of friction at the interfaces of the specimens and the compression machine was unnecessary. Contributions from elastic deformation of the specimen and machine parts and local adjustment of the specimens to the compression machine were corrected by calculating the inelastic strain for stresses >100 MPa as $\varepsilon = \varepsilon_{tot} - \varepsilon_{tot}\ (100\ MPa) - \sigma/E_{eff}$, where $E_{eff} = 45$ GPa is the effective elastic modulus determined from the steepest slopes of the loading parts of the σ–ε_{tot} curves. The microstructure was investigated by transmission electron microscopy (TEM) (Philips CM200). The subgrain intercepts were determined from montages of TEM micrographs (three montages, total area > 360 μm² per state) by the line intersection technique; the average intercept length is the subgrain size w.

Figure 2 shows the σ–ε history in the TMT of the type proposed in Ref. [3] to stabilize the UFG structure. It involves steps of deformation up to the peak of flow stress at constant $\dot{\varepsilon}_{tot}$ and temperature T in a sequence of increasing T up to 393 K.

During deformation at 403 K the TMT-stabilized UFG Cu softens (Fig. 3) like that in Figure 1. TEM investigations of the microstructure were done before TMT in the initial state after SPD and after TMT at points 1 (near maximum flow stress) and 2 (after work softening) of Figure 3. Figure 4 presents the results. It is known that the subgrain size w is usually close to its steady-state value in coarse-grained material, and depends on stress as $w_\infty = k_w bG/\sigma$, where b is the length of the Burgers vector, G is the shear modulus [15], and

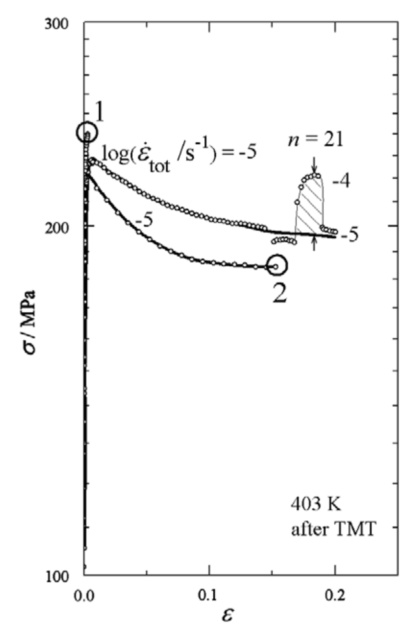

Figure 3. σ–ε curves at 403 K for UFG Cu after TMT of Figure 2 (curves ending at points 1 and 2 follow upper and lower curves from Fig. 2). Exponent n was determined from the change in flow stress with rate, marked by arrows.